Three-dimensional Retinal Imaging with High-Speed Ultrahigh-Resolution Optical Coherence Tomography

Maciej Wojtkowski, PhD,[1,2] *Vivek Srinivasan, MS,*[1] *James G. Fujimoto, PhD,*[1] *Tony Ko, MS,*[1] *Joel S. Schuman, MD,*[3] *Andrzej Kowalczyk, PhD,*[4] *Jay S. Duker, MD*[2]

Purpose: To demonstrate high-speed, ultrahigh-resolution, 3-dimensional optical coherence tomography (3D OCT) and new protocols for retinal imaging.

Methods: Ultrahigh-resolution OCT using broadband light sources achieves axial image resolutions of ~2 μm compared with standard 10-μm-resolution OCT current commercial instruments. High-speed OCT using spectral/Fourier domain detection enables dramatic increases in imaging speeds. Three-dimensional OCT retinal imaging is performed in normal human subjects using high-speed ultrahigh-resolution OCT. Three-dimensional OCT data of the macula and optic disc are acquired using a dense raster scan pattern. New processing and display methods for generating virtual OCT fundus images; cross-sectional OCT images with arbitrary orientations; quantitative maps of retinal, nerve fiber layer, and other intraretinal layer thicknesses; and optic nerve head topographic parameters are demonstrated.

Results: Three-dimensional OCT imaging enables new imaging protocols that improve visualization and mapping of retinal microstructure. An OCT fundus image can be generated directly from the 3D OCT data, which enables precise and repeatable registration of cross-sectional OCT images and thickness maps with fundus features. Optical coherence tomography images with arbitrary orientations, such as circumpapillary scans, can be generated from 3D OCT data. Mapping of total retinal thickness and thicknesses of the nerve fiber layer, photoreceptor layer, and other intraretinal layers is demonstrated. Measurement of optic nerve head topography and disc parameters is also possible. Three-dimensional OCT enables measurements that are similar to those of standard instruments, including the StratusOCT, GDx, HRT, and RTA.

Conclusion: Three-dimensional OCT imaging can be performed using high-speed ultrahigh-resolution OCT. Three-dimensional OCT provides comprehensive visualization and mapping of retinal microstructures. The high data acquisition speeds enable high-density data sets with large numbers of transverse positions on the retina, which reduces the possibility of missing focal pathologies. In addition to providing image information such as OCT cross-sectional images, OCT fundus images, and 3D rendering, quantitative measurement and mapping of intraretinal layer thickness and topographic features of the optic disc are possible. We hope that 3D OCT imaging may help to elucidate the structural changes associated with retinal disease as well as improve early diagnosis and monitoring of disease progression and response to treatment. *Ophthalmology 2005;112:1734–1746 © 2005 by the American Academy of Ophthalmology.*

Over the past 10 years, optical coherence tomography (OCT) has emerged as a new technique that can provide high-resolution cross-sectional images of the retina for identifying, monitoring, and quantitatively assessing diseases of the macula and optic nerve head.[1–4] A commercial system, the StratusOCT (Carl Zeiss Meditec, Dublin, CA), with an axial resolution of 10 μm has been developed. Optical coherence tomography techniques that provide 3-dimensional (3D) information, including fundus images, have also been developed.[5–8] Recently, ultrahigh-resolution OCT (UHR OCT) imaging with axial

Originally received: November 30, 2004.
Accepted: May 16, 2005. Manuscript no. 2004-352.

[1] Department of Electrical Engineering and Computer Science and Research Laboratory of Electronics, Massachusetts Institute of Technology, Cambridge, Massachusetts.

[2] New England Eye Center, Tufts–New England Medical Center, Tufts University, Boston, Massachusetts.

[3] UPMC Eye Center, Department of Ophthalmology, Eye and Ear Institute, University of Pittsburgh School of Medicine, Pittsburgh, Pennsylvania.

[4] Institute of Physics, Nicolaus Copernicus University, Torun, Poland.

Presented, in part, at: Association for Research in Vision and Ophthalmology meeting, May, 2004; Fort Lauderdale, Florida.

Supported in part by National Institutes of Health, Bethesda, Maryland (grant nos.: R01-EY11289-19, R01-EY13178-05, P30-EY008098); National Science Foundation, Arlington, Virginia (grant no.: ECS-0119452); Medical Free Electron Laser Program, Air Force Office of Scientific Research, Arlington, Virginia (contract no.: F49620-01-1-0186); The Eye and Ear Foundation, Pittsburgh, Pennsylvania; and an unrestricted grant from Research to Prevent Blindness, New York, New York.

Drs Fujimoto and Schuman receive royalties from intellectual property licensed by the Massachusetts Institute of Technology to Carl Zeiss Meditec.

Correspondence to James G. Fujimoto, PhD, Department of Electrical Engineering and Computer Science and Research Laboratory of Electronics, Massachusetts Institute of Technology, 77 Massachusetts Avenue, Cambridge, MA, 02139. E-mail: jgfuji@mit.edu.

ISSN 0161-6420/05/$–see front matter
doi:10.1016/j.ophtha.2005.05.023

resolutions of ~3 μm has been demonstrated; this technique significantly improves the visualization of retinal morphology.[9–13] Improved axial resolution enables the visualization and measurement of intraretinal layers such as photoreceptor, ganglion cell, plexiform, and nuclear.

The total permissible image acquisition time for any OCT system is limited by subject eye motion, which can cause image artifacts. Because standard OCT systems have limited image acquisitions speeds, comprehensive 3D imaging of the retina was not previously possible. Instead, specialized OCT diagnostic protocols were developed to image and assess quantitatively the macula and peripapillary region and optic nerve head.[2,14,15] Assessment of these areas involves the acquisition of a small set of individual OCT images with a given scan pattern and, therefore, does not provide comprehensive coverage of the retina. Thus, focal areas of pathology can be missed. Imaging speeds in conventional UHR OCT are slower than those in standard-resolution OCT, so the coverage of the retina is even more restricted.

Recently, dramatic advances in OCT technology have enabled OCT imaging with a ~15-times to 50-times increase in imaging speed over standard-resolution OCT systems and ~100-times increase over UHR OCT systems.[16–20] These novel detection techniques are known as Fourier domain or spectral detection techniques, because echo time delays of light are measured by taking the Fourier transform of the interference spectrum of the light signal.[21,22] Different echo time delays of light produce different frequencies of fringes in the interference spectrum. A Fourier transform is a mathematical procedure that extracts the frequency spectrum of a signal. Because OCT with spectral/Fourier domain detection can measure all echoes of light from different delays simultaneously, it has a dramatic speed and sensitivity advantage compared with OCT using standard detection. Using OCT with spectral/Fourier domain detection, it is possible to acquire complete 3D data sets in a time comparable to that of current OCT protocols that acquire several individual images. In vivo OCT imaging of the retina with 10-μm axial resolution using OCT spectral/Fourier domain detection was demonstrated in 2002.[23] High-speed retinal and anterior eye imaging with an exposure time of only 64 microseconds per axial scan was shown in 2003.[24] Video-rate OCT imaging with acquisition speeds of 29 000 axial scans per second and 6-μm axial resolution was reported in 2004.[16] High-speed UHR retinal imaging with 3.5-μm axial resolution at 15 000 axial scans per second,[25] 2.5-μm axial resolution at 10 000 axial scans per second,[17] and 2.1-μm axial resolution at 16 000 axial scans per second[18] was demonstrated in the same year.

In this article, high-speed UHR OCT using spectral/Fourier domain detection is demonstrated for 3D volumetric imaging of the retina (3D OCT). This research prototype system achieves a ~2-μm axial image resolution, a 5-times improvement in axial image resolution versus standard ~10-μm-resolution OCT with imaging speeds that are ~40 times faster than standard StratusOCT. A raster scan imaging protocol, which acquires consecutive OCT images at equally spaced lateral intervals, is used to obtain 3D OCT data. The number and density of axial scans on the retina are dramatically increased relative to standard OCT. This reduces sampling errors and the possibility of missing focal pathologies. An OCT fundus image can be generated directly from the 3D OCT data by integrating the OCT signal in the axial direction. This OCT fundus image enables precise and repeatable registration of OCT cross-sectional images with fundus features. Optical coherence tomography fundus images of individual intraretinal layers can also be generated. Because it is possible to acquire high-density volumetric data of the macula or optic disc, 3D OCT data can be processed to provide comprehensive structural information about the retina. Optical coherence tomography images with arbitrary orientation and position, such as circumpapillary scans, can be generated directly from the 3D OCT data. Quantitative mapping of retinal layers, including measurements of the thicknesses of the retina, retinal nerve fiber layer (RNFL), photoreceptor layer, and other intraretinal layers, can be performed. Topographic parameters of the optic nerve head and disc can be measured. High-speed UHR 3D OCT can be used to measure retinal structure and topography in a manner similar to that of other imaging modalities such as the GDx (Laser Diagnostic Technology, San Diego, CA), HRT (Heidelberg Engineering GmbH, Heidelberg, Germany), and RTA (Talia Technology Ltd., Lod Industrial Area, Israel).

Materials and Methods

Classic OCT systems perform measurements of the echo time delay of backscattered or backreflected light by using an interferometer with a mechanically scanned optical reference path.[1,2,26] Measurements of the echo delay and magnitude of light are performed by mechanically scanning the reference path length so that light echoes with sequentially different delays are detected at different times as this reference path length is scanned. For this reason, these systems are known as time domain systems. Standard clinical ophthalmic OCT instruments such as the StratusOCT have scanning speeds of 400 axial scans per second and, therefore, can acquire a 512–axial scan (transverse pixel) OCT image in ~1.3 seconds. Higher scan speeds of up to several thousand axial scans per second have been achieved by using more advanced methods of mechanical scanning, and high-speed imaging in other applications such as endoscopy has been demonstrated.[27,28] However, the detection sensitivity of any OCT system decreases with increased imaging speed.[29] Because the permissible light exposure levels in the eye are limited and light signals from the retina are extremely weak, retinal imaging speeds have been limited.

New detection techniques known as spectral/Fourier domain detection can dramatically improve the sensitivity and imaging speed of OCT.[30–32] Spectral/Fourier domain detection techniques measure the echo time delay of light by measuring the spectrum of the interference between light from the tissue and light from a stationary unscanned reference arm. Fourier detection uses a spectrometer and a high-speed charge coupled device linescan camera to measure the interference spectrum. The echo time delays of the backscattered or backreflected light from the tissue can be measured by taking the Fourier transform of the interference spectrum, hence the name spectral/Fourier domain detection. The result is a measurement of echo time delay and magnitude of light analogous to the axial scan mea-

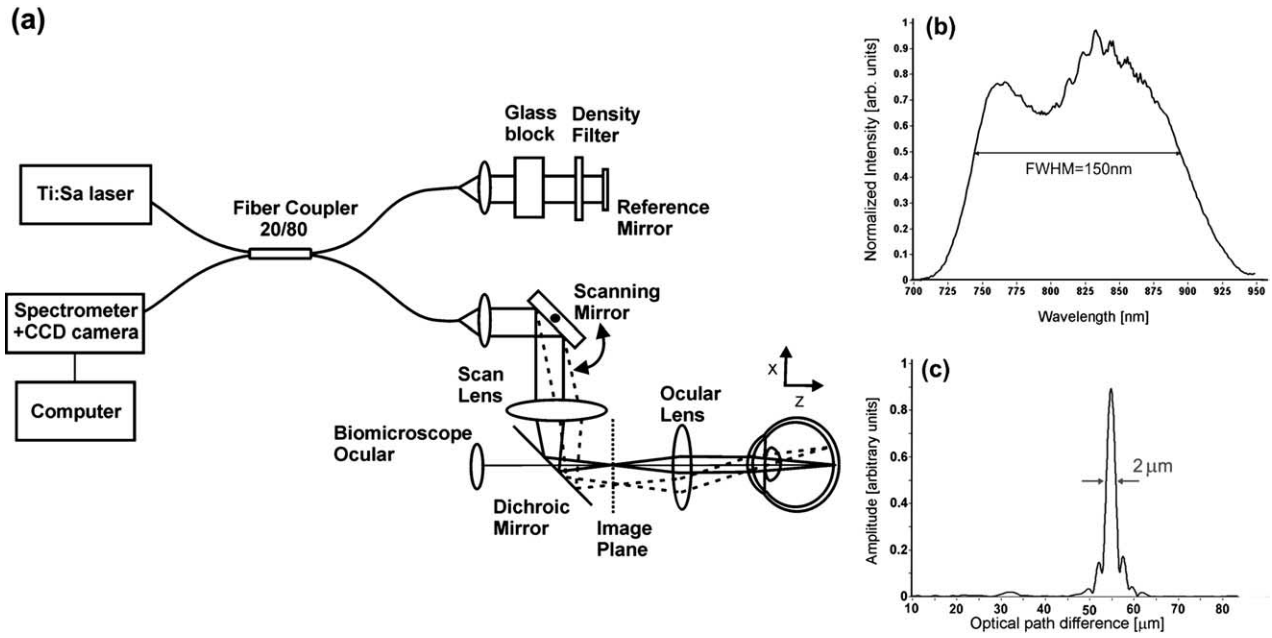

Figure 1. Schematic of high-speed ultrahigh-resolution optical coherence tomography system using spectral/Fourier domain detection (**a**). Echo time delays and magnitudes of backscattered or backreflected light are detected by measuring the spectrum of the interferometer output. A femtosecond laser light source generates broad bandwidths necessary to achieve ultrahigh axial image resolutions. The bandwidth of the light source is 150 nm (**b**), achieving an axial resolution of 2 μm in the retina (**c**). CCD = charge coupled device; FWHM = full width at half maximum; Ti:Sa = titanium:sapphire.

surements in classic OCT, except that scanning of the reference arm is not required. Because all of the light echoes from different axial positions in the sample are measured simultaneously, rather than sequentially, detection sensitivity and imaging speed can be increased dramatically.

The axial (longitudinal) image resolution of OCT is determined by a property of the light source known as the coherence length, which is inversely proportional to the bandwidth ($\Delta\lambda$) of the light source. The axial resolution is given by the equation $\Delta L = 2\ln(2)\lambda^2/(\pi\Delta\lambda)$, where ($\Delta\lambda$) is the bandwidth and ($\lambda$) is the central wavelength of the light source. To improve axial resolution, broad-bandwidth light sources are required. In our experiments, we used a state-of-the-art femtosecond titanium: sapphire laser light source for imaging.[9,10] Optical components in the interferometer and retinal imaging system were designed to support a broad-spectral bandwidth. As shown in Figure 1, the bandwidth of the light source was 150 nm full width at half maximum, yielding a measured axial image resolution of 2.6 μm in air, corresponding to ~2 μm in the retina.[18] The current research instrument was redesigned to improve the bandwidth and has finer resolution than previous UHR OCT research instruments with ~3-μm resolutions.[16–19] In addition, the use of spectral/Fourier domain detection enables precise compensation of dispersion, which was a limiting factor in previous systems.

Figure 1 shows a schematic of the high-speed UHR OCT research prototype system using spectral/Fourier domain detection. A detailed description of the system has been given.[18] A broadband titanium:sapphire laser is used as the light source for a fiber optic interferometer.[10] Light in the reference arm is attenuated and reflected from a stationary mirror at a fixed delay. Light in the sample arm is directed though 2 galvanometer-actuated steering mirrors and relay imaged through the pupil onto the retina.[2] The galvanometer actuated mirrors scanned the OCT imaging beam on the retina. The incident light on the eye was 750 μW, the same exposure used in commercial ophthalmic OCT systems, consistent with American National Standards Institute safety standards. The spectrum of the interferometer output was detected using a spectrometer consisting of a collimating lens, transmission grating, imaging lens, and charge coupled device linescan camera. The charge coupled device linescan camera had 2048 pixels and was read at a 40-megahertz pixel reading rate. The reading rate specifies the maximum rate at which data can be transferred from the camera, but does not include the exposure time. The interference spectrum data from the camera was transferred to computer system memory (3.2-gigahertz Pentium IV), where it was rescaled from wavelength to frequency and Fourier transformed to generate axial measurements of the echo delay and magnitude of light from the retina. Three-dimensional data sets were acquired by scanning the OCT beam on the retina under computer control. These studies were approved by the Massachusetts Institute of Technology Committee on the Use of Humans as Experimental Subjects and the institutional review boards of the Tufts–New England Medical Center and the University of Pittsburgh School of Medicine.

Our prototype high-speed UHR OCT system enables data acquisition rates of up to 16 000 axial scans per second, corresponding to acquiring >30 images (of 512 axial scans/transverse pixels each) per second. The net data acquisition rate is determined by a combination of the number of pixels in each axial scan, the spectrometer linescan camera exposure time required to achieve sufficient sensitivity, the camera reading rate, and the maximum speed with which the galvonometers can scan the desired pattern. Data processing is required to generate axial scan information from the spectral interference measurement. Real-time display could be performed at up to 18 images (of 512 axial scans each) per second using only the computer software, without the need for specialized hardware. This rate is sufficient to provide a flicker-free display and enable focusing and alignment of the OCT instrument. Finally, it is important to note that the real-time display does not impede data acquisition: data may be acquired at the maximum rate while simultaneously displaying at a slower rate.

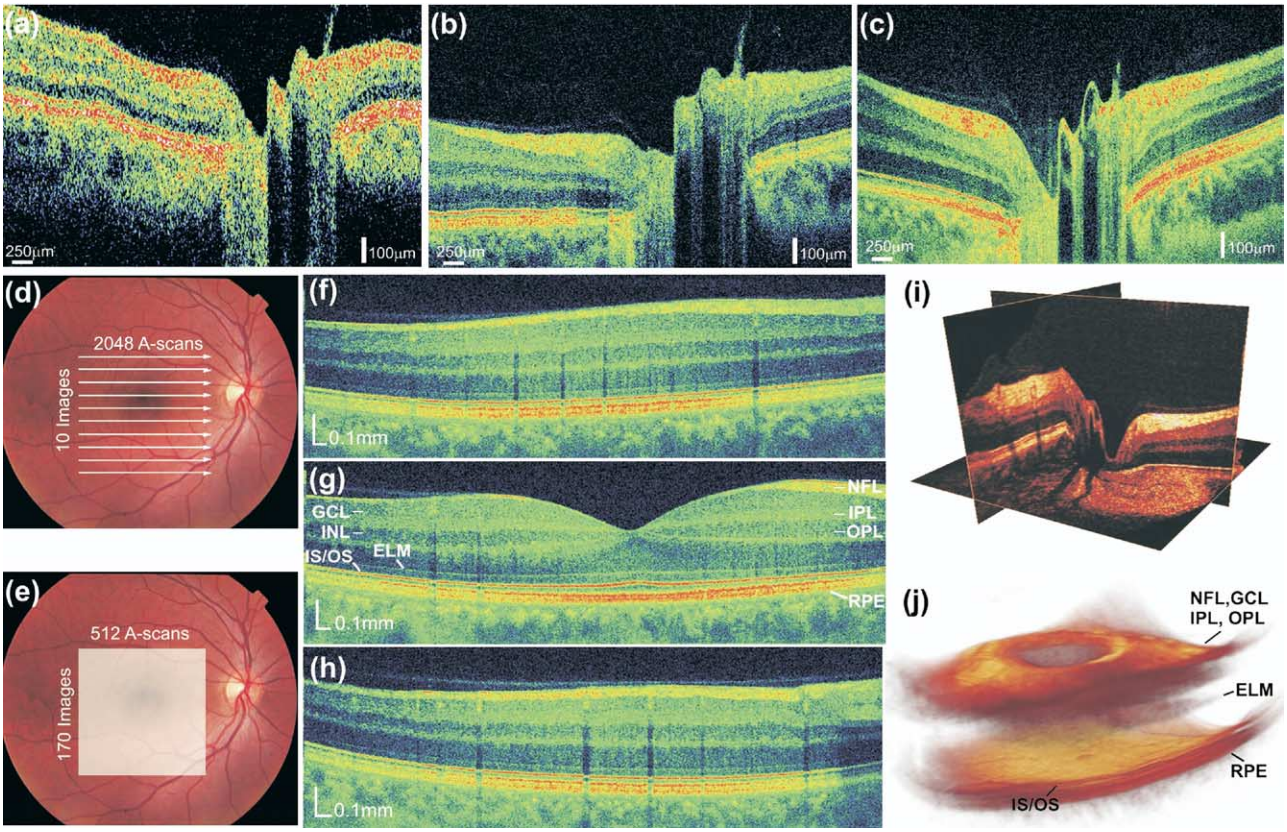

Figure 2. Comparison of normal optic nerve head imaged with different optical coherence tomography (OCT) technologies. **a**, Standard-resolution OCT image with axial resolution of ~10 μm, 512 transverse pixels (axial scans), acquired in ~1.3 seconds. **b**, Ultrahigh-resolution (UHR) OCT image with axial resolution of ~3 μm, 600 transverse pixels, acquired in ~4 seconds. **c**, High-definition image using high-speed UHR OCT with axial resolution of ~2 μm, 2048 transverse pixels, acquired in 0.13 seconds. High-speed imaging enables raster scan patterns for comprehensive 3-dimensional mapping of the retina (3D OCT). Examples of 2 different scan patterns are shown: (**d**) 10 cross-sectional images with 2048 axial scans (transverse pixels) each for high-definition imaging, (**e**) 170 images with 512 axial scans each for 3D OCT imaging, (**f–h**), representative high-definition OCT images of the macula, (**i**) representative cross-sectional images along orthogonal planes of the optic disc generated from the 3D OCT data set, and (**j**) volume rendering of the macula from the 3D OCT data. ELM = external limiting membrane; GCL = ganglion cell layer; INL = inner nuclear layer; IPL = inner plexiform layer; IS/OS = boundary between the inner and outer segments of the photoreceptors; NFL = nerve fiber layer; OPL = outer plexiform layer; RPE = retinal pigment epithelium.

Results

To compare image quality from different OCT systems, images of the normal optic nerve head were acquired with standard-resolution OCT using the StratusOCT, UHR OCT using an earlier research prototype instrument, and high-speed UHR OCT using the current research prototype instrument, as shown in Figure 2a–c. The standard-resolution OCT image has an axial resolution of ~10 μm in tissue, consists of 512 transverse pixels (axial scans), and is acquired in ~1.3 seconds. The UHR OCT image has an axial resolution of ~3 μm, consists of 600 transverse pixels, and is acquired in ~4 seconds.[9–13] The high-speed UHR OCT image has an axial resolution of ~2 μm, consists of 2048 transverse pixels, and is acquired in 0.13 seconds. The images are displayed with an expanded axial scale to facilitate better visualization of the retinal layers. Comparing UHR OCT with standard-resolution OCT shows that the improved axial image resolution improves the visualization of retinal morphology, allowing visualization of intraretinal layers. Comparing the high-speed UHR OCT with the UHR OCT shows that the increased transverse pixel (axial scan) density further improves image quality. Motion artifacts can be seen in the standard-resolution OCT image. The UHR OCT image has been cross-correlated using standard algorithms to remove motion artifacts, but this results in the loss of topographic information. The high-speed UHR OCT image is acquired so rapidly that motion artifacts are not present, and topographic information is correctly preserved.

Standard OCT instruments such as the StratusOCT use specific imaging protocols for measuring macular thickness, RNFL thickness, and optic nerve head parameters.[4] Six OCT images oriented radially at different clock hours are used to map the macula.[2,15] Three repeated circumpapillary scans around the optic nerve head are used for measuring nerve fiber layer (NFL) thickness.[14,33] Six OCT images oriented radially at different clock hours are used to map the optic nerve head and determine disc parameters.[2] Specialized imaging protocols involving the acquisition of a few individual OCT images are required because of the acquisition speed limitations in standard OCT. With the development of new high-speed UHR OCT, it is possible to use a raster scan to obtain comprehensive 3D volumetric data of the retinal structure. The raster scan protocol also has the advantage of sampling the retina on a rectangular grid, providing simple reconstruction and uniform coverage. Raster scanning is used in other clinical imaging instruments such as the GDx, HRT, and RTA.

Figure 2d, e also shows examples of 2 raster scan protocols, each covering a 6 × 6-mm-square area of the fundus. The first scan protocol acquires 10 images with 2048 axial scans (transverse pixels) × 1024 axial pixels and is used to acquire a set of high-definition OCT images. Using our current research prototype system, the image acquisition time is 0.13 seconds per image, and all 10 images are acquired in ~1.3 seconds. These are high-definition images with a high transverse pixel density with an axial scan (transverse pixel) spacing of 2.9 μm (6 mm/2048) on the retina; they enable improved visualization of intraretinal layers relative to standard OCT images, which typically have 512 axial scans (transverse pixels). Each of the 10 individual horizontal OCT images is offset by 600 μm (6 mm/10) in the vertical on the retina. The axial range (depth range) is 1 mm, so the 1024 axial pixels have a spacing of 1 μm (1 mm/1024) in depth. The ultrahigh axial resolution enables improved visualization of individual layers of the retina including the NFL, ganglion cell layer (GCL), inner and outer plexiform layers, inner nuclear layer, outer nuclear layer (ONL), and retinal pigment epithelium (RPE). Features such as the reflection from the boundary between the inner and outer segments of the photoreceptors and the external limiting membrane can also be visualized.

The second scan protocol acquires 170 images with 512 axial scans (transverse pixels) × 1024 axial pixels and is used to acquire 3D volumetric data of the retinal structure. The data acquisition time is 6 seconds using our current research prototype system. If a smaller area of the retina is imaged, or as imaging speeds improve, the image acquisition time can be decreased accordingly. The scan protocol of 170 images of 512 pixels each was chosen so that a set of standard-quality OCT images were produced in the horizontal direction. These images have transverse pixel spacing (spacing between axial scans) of 12 μm (6 mm/512), similar to standard-quality OCT images. The 170 horizontal images are spaced by 35 μm (6 mm/170) in the vertical direction on the retina. Although this scan protocol results in asymmetric axial scan spacing in the horizontal and vertical directions, it has the advantage that individual horizontal OCT images can be selected for display. Automated segmentation for measuring retinal layer thickness can be performed more readily on images with high transverse pixel densities. The raster scan protocol uses horizontal scans, following the convention of the StratusOCT; however, a scan protocol using vertically rather than horizontally oriented scans can also be performed.

The 3D data set consists of 87 040 axial scans (512 × 170) that sample the retina on a rectangular grid with a spacing of 12 × 35 μm (horizontal × vertical) over a 6 × 6-mm area. This provides a comprehensive volumetric coverage of the retina and enables rendering and mapping. The thickness of the retina or intraretinal layers can be measured by applying segmentation algorithms similar to those previously developed for standard-resolution OCT images.[10,14,15] Both raster scan protocols have the advantage that they measure a larger number of transverse points on the retina than standard-resolution OCT, thus reducing the possibility that focal pathologies will be missed in the OCT images or in mapping.

Volume Rendering of 3-dimensional Optical Coherence Tomography Data

To visualize the 3D retinal structure, 3D OCT data sets can be rendered volumetrically, as shown in Figure 2i, j. Before rendering, the individual cross-sectional OCT images in the 3D data set were correlated automatically and aligned by software to remove axial eye motion artifacts that caused variations in the axial position of the retina between images. Standard OCT imaging requires cross-correlation between axial scans within an image.[26] However, for the data presented here, cross-correlation between consecutive axial scans within an image is not necessary because the high image acquisition speed makes eye motion during an individual OCT image negligible. The 3D data were rendered using image processing software similar to that used in magnetic resonance image processing.

Figure 2i shows orthogonal slices or an orthoplane rendering of the 3D OCT data. The images correspond to an area of 6 × 6 mm and a depth of 1 mm. In this example, a raster imaging protocol consisting of 170 horizontally oriented images of 512 transverse pixels each was used to generate the 3D OCT data. Therefore, horizontal OCT images will consist of 512 transverse pixels, whereas vertical OCT images will consist of 170 transverse pixels. Optical coherence tomography images can be generated with arbitrary orientations from 3D OCT data but will have varying transverse resolutions depending on the direction of the scan and the density of the initial 3D OCT data set.

In addition, volume rendering and other visualization methods may also be applied. Figure 2j shows a rendering of selected macular layers including the NFL, GCL, inner and outer plexiform layers, external limiting membrane, inner/outer photoreceptor junction, and the RPE. The image corresponds to an area of 6 × 6 mm with a depth of 1 mm. Other retinal regions and complexes of layers can also be rendered using 3D OCT data. Although there is currently no clinical application for this type of visualization, these methods are well accepted in magnetic resonance imaging. The ability to visualize 3D morphology may be helpful in fundamental research applications for elucidating structural changes in retinal disease or for future clinical applications, such as planning epiretinal membrane surgery.

Optical Coherence Tomography Fundus Image Generation and Registration of Optical Coherence Tomography Images

Clinical OCT systems use standardized OCT imaging protocols that scan specific areas of the fundus. A video fundus photograph is taken immediately after the OCT images are acquired in order to show the position of the OCT scans. However, it can be difficult to ensure that OCT images are registered precisely with respect to specific fundus features. In addition, image information on focal pathologies is not obtained if the appropriate fundus location is not scanned. Precise and reproducible control of the OCT image position on the fundus is especially important for morphometry, such as measurement of NFL thickness in glaucoma diagnosis. Three-dimensional en-face OCT imaging techniques have been developed that simultaneously perform OCT imaging and scanning laser ophthalmoscopy, thereby enabling precise registration to fundus landmarks.[6,34,35] These systems acquire excellent fundus images, but axial resolution is limited compared with standard OCT because relatively small numbers of transverse (en face) images are obtained and used to construct axial image information.

An OCT view of the fundus can be produced directly from 3D OCT data, as shown schematically in Figure 3a–c. This OCT fundus image is similar to that obtained by fundus photography or scanning laser ophthalmoscopy and enables the precise registration of OCT image data with fundus features because the OCT fundus images and OCT cross-sectional images are generated from the same data set. The OCT fundus image is generated by summing the 3D OCT data along the axial direction at each transverse point on the retina. This generates a brightness value for each axial scan, at each transverse position on the retina, which corresponds to the total backscattering or backreflected light from all of the retinal layers at that position. Figure 3d is an example of an OCT fundus image displayed in grayscale. This OCT fundus image was generated from 3D OCT data using the previously described raster

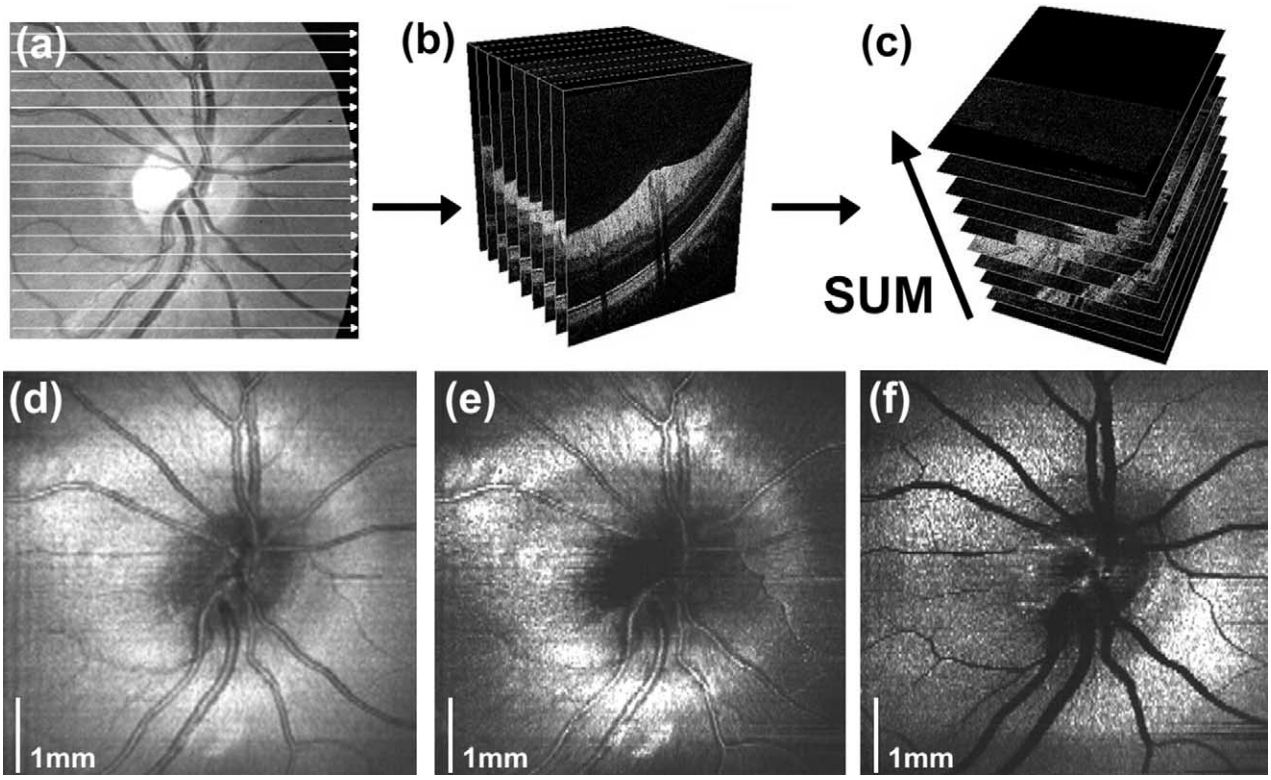

Figure 3. a–c, An optical coherence tomography (OCT) fundus image can be generated directly from 3-dimensional OCT data by summing the signal along the axial direction. **d**, The OCT fundus image provides an en face view that is equivalent to a fundus photograph. The OCT fundus image enables individual OCT images to be registered precisely to fundus features because they are generated from the same data set. Optical coherence tomography fundus images can also be generated by displaying individual retinal layers such as (**e**) the nerve fiber layer or (**f**) retinal pigment epithelium.

scan protocol, and consists of 512 × 170 pixels (horizontal × vertical).

It is also possible to generate OCT fundus images that selectively display specific retinal layers or specific retinal features. Figure 3e, f also shows examples of OCT fundus images of the NFL and the RPE. These images were generated from 3D OCT data by summing and displaying the signals from inner and outer parts of cross-sectional images where scattering from the RPE and NFL layers is dominant. The OCT fundus image of the RPE exhibits enhanced contrast because of shadowing of the RPE by blood vessels. The RPE OCT fundus image shows the termination of the RPE at the disc margin and may be useful for mapping disruptions of the RPE. The OCT fundus image of the NFL shows variations that are correlated with the normal thickness variation of the NFL. The NFL OCT fundus image may be useful as an adjunct to NFL thickness mapping for visualizing NFL defects. Many other types of OCT fundus imaging are possible by displaying normalized ratios or other, more complex functions of the signals from different retinal layers.

The OCT fundus images can be correlated directly to a fundus photograph or any other imaging modality that provides a fundus view. Fixation changes during the raster scan can be identified by detecting discontinuities in blood vessels and other features on the virtual fundus image. This feature could be used either as a quality metric or to post process 3D OCT data to reduce or correct for eye motion artifacts. Because the OCT fundus image is generated directly from 3D OCT data, the OCT cross-sectional images are registered precisely to the fundus view. Thickness maps obtained by segmentation of 3D OCT data can also be overlaid in false color over the grayscale OCT fundus image.

Mapping Retinal Thicknesses

Measurement of retinal thickness is important for quantifying macular edema. Macular edema is a consequence of many conditions, such as diabetic retinopathy, epiretinal membrane formation, ocular inflammation, retinal vascular occlusion, and cataract extraction. Mapping of the retinal thickness in the macula is also important for the detection and monitoring of glaucoma.[36] Commonly used clinical instruments for measuring and mapping total retinal thickness include the RTA and OCT (StratusOCT).

The RTA performs measurements of retinal thickness using an elegant method somewhat similar to that used in slit-lamp biomicroscopy. A thin slit is generated using a visible laser and projected onto the retina at a known angle.[37,38] Images of the slit illumination of the front of the retina and the RPE are recorded and analyzed to measure the retinal thickness with an axial resolution of approximately 50 μm. The RTA can scan a 3 × 3-mm region of the retina using 16 optical cross-sections that are acquired in 0.3 seconds. The RTA generates thickness maps that are registered precisely to fundus photographs. Comparative studies between the RTA and OCT indicate that the instruments have similar performances in the measurement of mild to moderate edema.[39]

The StratusOCT performs measurements of macular thickness using 6 intersecting 6-mm-long OCT images oriented in a radial pattern centered on the fovea.[15] Six images of 128 axial scans (transverse pixels) each can be acquired in ~2 seconds, or 6 images of 512 axial scans (transverse pixels) each can be acquired in ~10 seconds. The radial scanning protocol was designed to concentrate measurements in the central fovea, where high sampling density is most important. The 6 OCT images are segmented to detect the retinal thickness, which is measured as the distance

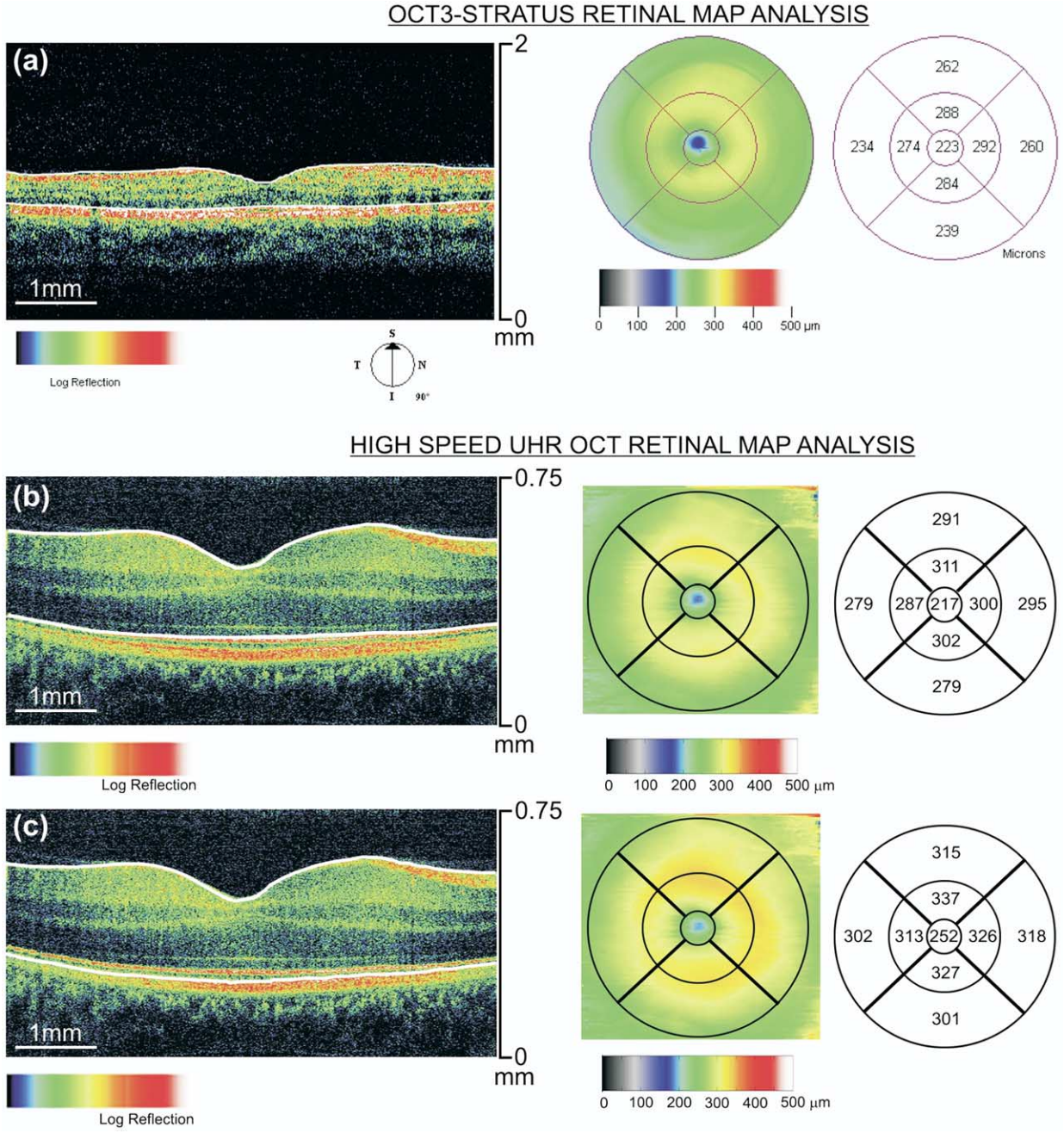

Figure 4. Comparison of false-color macular thickness maps obtained using (**a**) the commercial optical coherence tomography (StratusOCT) and (**b, c**) high-speed ultrahigh-resolution (UHR) 3-dimensional OCT. StratusOCT uses 6 intersecting 6.0-mm OCT images in a radial pattern centered on the fovea. Using OCT images with 512 transverse pixels, this corresponds to 3072 different transverse points on the retina. Three-dimensional OCT using high-speed UHR OCT maps the retinal thickness using a raster scan with 87 000 points. Retinal thickness maps are divided into 9 Early Treatment Diabetic Retinopathy Study–type regions, and the average thickness for each region is displayed. Ultrahigh-resolution OCT can distinguish the junction between the inner and outer segments of the photoreceptors (IS/OS) separately from the retinal pigment epithelium (RPE). Therefore, it is possible to measure an effective retinal thickness from the IS/OS as in StratusOCT (b) versus the actual retinal thickness from the RPE (c).

from the photoreceptor inner/outer segment junction to the vitreal retinal interface. The retinal thickness is displayed as a false-color topographic map, as shown in Figure 4a. The thickness maps are divided into 9 Early Treatment Diabetic Retinopathy Study–type regions, and the average thickness value for each region is displayed. Because the radial pattern of 6 OCT images samples the macular thickness along clock hours, the retinal thickness in the wedges between each image is interpolated. Therefore, this imaging protocol may miss pathologies such as focal edema located in a span of <1 clock hour, or 30°.

The 3D OCT data can be processed using segmentation algorithms to detect boundaries between different layers of the retina and to map the thickness of different retinal layers quantitatively.[10,14,15] High-speed UHR OCT images have higher resolution

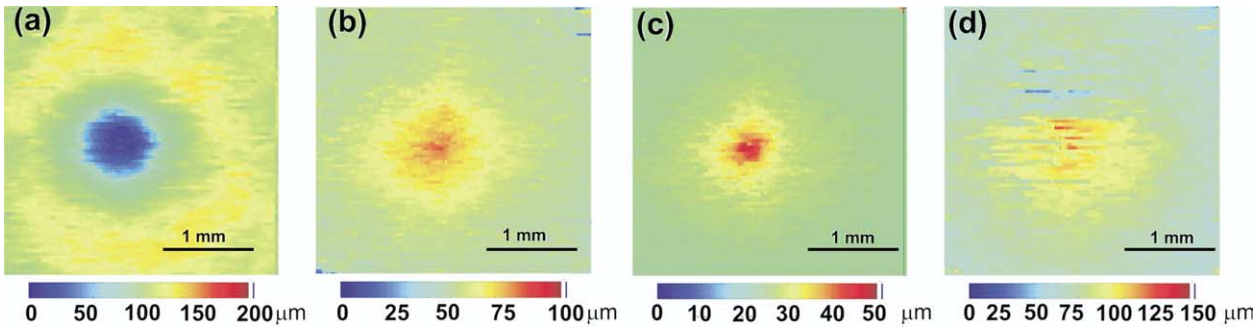

Figure 5. Three-dimensional optical coherence tomography enables mapping of the thickness of individual intraretinal layers: (**a**) combined thickness of ganglion cell layer, inner plexiform layer, and nerve fiber layer; (**b**) distance from external limiting membrane to retinal pigment epithelium (RPE); (**c**) distance from the photoreceptor inner segment/outer segment junction to the RPE; and (**d**) outer nuclear layer thickness. Maps b–d are useful for quantitative measurement of photoreceptor changes.

than standard OCT images, and this improves the performance of segmentation or other image-processing algorithms. Ultrahigh-resolution OCT allows improved visualization and quantitative mapping of intraretinal layers, such as with features in the photoreceptors, compared with standard-resolution OCT. Three-dimensional OCT imaging using high-speed UHR OCT enables much more comprehensive coverage of the retina than standard OCT. Using the raster scan protocol previously described in "Materials and Methods," the retinal thickness is measured at 87 000 points on a rectangular grid with a spacing of 12 × 35 μm (horizontal × vertical) over a 6 × 6-mm retinal area. In comparison, the standard OCT imaging protocol of 6 radial OCT scans has an axial scan spacing of up to 1.6 mm at the outer perimeter of the circle.

As noted previously, a raster scan with asymmetric spacing of the axial scans (transverse pixels) was chosen to yield good OCT images in the horizontal direction. However, a raster scan consisting of 300 × 300 axial scans (horizontal × vertical) over a 6 × 6-mm retinal area, corresponding to a square grid with an axial scan spacing of 20 × 20 μm, can also be obtained in a comparable acquisition time. Image acquisition times can also be shortened by reducing the size of the area imaged. A 3 × 3-mm retinal area can be imaged 4 times faster than a 6 × 6-mm area.

Figure 4 shows a comparison of retinal thickness maps obtained using the StratusOCT and 3D OCT data from the high-speed UHR OCT system. Ultrahigh-resolution OCT enables differentiation of the junction between the inner and outer segments of the photoreceptors as a distinct feature from the RPE. Therefore, 2 versions of the retinal thickness map are presented. Figure 4b shows a thickness map that measures the distance from the junction between the inner and outer segments of the photoreceptors to the vitreal retinal interface, which agrees closely with the map obtained using the StratusOCT, shown in Figure 4a. Figure 4c shows a thickness map that measures the retinal thickness as the distance from the inner interface of the hyporeflective band corresponding to the RPE to the vitreal retinal interface. This more closely corresponds to the actual anatomical retinal thickness.

Mapping Intraretinal Layers

In addition to the total retinal thickness, it is also possible to image and map intraretinal layers using 3D OCT data from high-speed UHR OCT. Mapping the thickness of the GCL in the macula could provide a sensitive method for the detection and monitoring of glaucoma because thinning of the GCL would accompany atrophy of the retinal nerve fibers.[36] Recent clinical studies with UHR OCT have demonstrated changes in photoreceptor morphology associated with disease and suggest that mapping of photoreceptor layer thicknesses could be used to assess photoreceptor integrity or impairment in disease.[11]

Figure 5 shows examples of intraretinal layer thickness maps obtained using 3D OCT. Figure 5a shows a map of the combined thickness of the GCL, inner plexiform layer, and NFL. This combination of retinal layers provides good contrast and can be segmented and measured more reliably than the GCL alone. This map may be useful for glaucoma diagnosis and monitoring. In the future, with higher density raster scans and improved algorithms, it should be possible to segment the GCL separately. Figure 5b shows a map of the thickness from the external limiting membrane to the RPE. Figure 5c shows a map of the thickness from the junction between the photoreceptor inner and outer segments to the RPE. These maps provide quantitative information on the photoreceptors that may be useful for assessing photoreceptor integrity or impairment. This mapping modality may be useful for monitoring diseases such as age-related macular degeneration, retinitis pigmentosa, or other degenerative diseases. Figure 5d shows the thickness of the ONL. The boundary of the ONL with the outer plexiform layer is relatively low contrast, so it is difficult to segment the ONL accurately, and a segmentation error can be seen in the map as a discontinuity in layer thickness.

Mapping the Nerve Fiber Layer

Quantitative measurements of the RNFL thickness and optic disc topography are important for the diagnosis and monitoring of glaucoma. Clinical instruments for measuring and mapping RNFL thickness include the scanning laser polarimeter (GDx) and OCT (StratusOCT). It has been shown that the GDx and OCT have comparable abilities to discriminate between healthy eyes and eyes with early to moderate glaucomatous visual field loss.[40]

The GDx measures the NFL by using scanning laser polarimetry, measuring the net birefringence on the NFL, which is correlated with its thickness. The GDx is similar to a scanning laser ophthalmoscope, but illuminates the retina with different polarizations of light and quantitatively measures the change in polarization when the light travels through the NFL and is retroreflected from the RPE.[41] The GDx generates an image of the fundus with a false-color map of NFL thickness. A 20° × 20° area of the retina can be imaged in <1 second. The GDx has the advantage of rapid imaging speed and generates a color map of NFL thickness that is registered to the fundus image (Fig 6a). The entire optic disc region is mapped, and it is possible to obtain quantitative graphs of the NFL thickness along any set of points, such as a circle centered on the optic nerve head, as shown in Figure 6b.

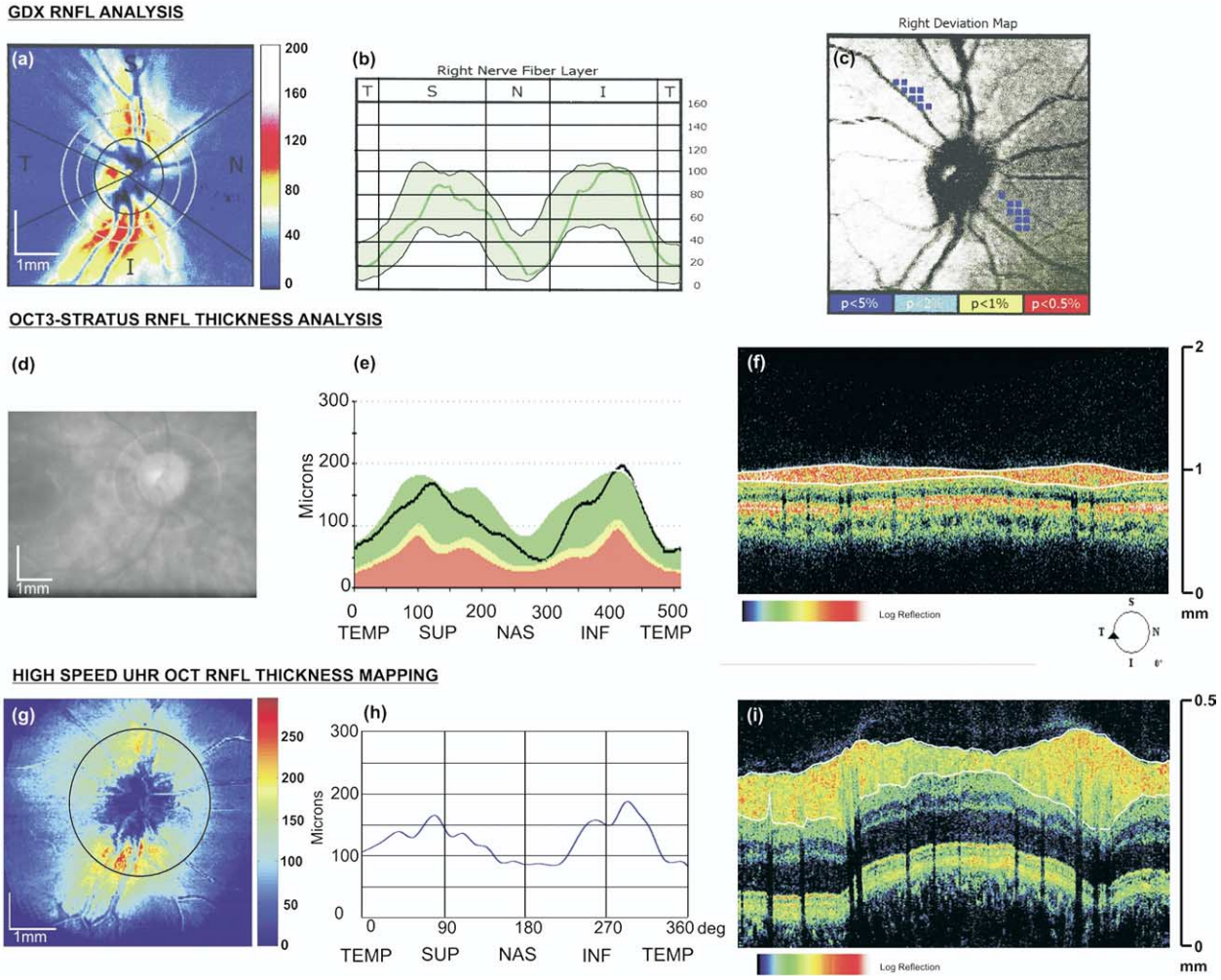

Figure 6. Comparison between retinal nerve fiber layer (RNFL) analysis obtained using GDx VCC, StratusOCT, and 3-dimensional optical coherence tomography (3D OCT): (**a, g**) false-color maps of RNFL thickness from GDx and 3D OCT; (**b, e, h**) plots of RNFL thickness on a 3.4-mm diameter circumpapillary ring from GDx, StratusOCT3, and 3D OCT; (**c**) GDx RNFL deviation map; (**d**) StratusOCT fundus photograph; (**f**) StratusOCT circumpapillary image; and (**i**) virtual circumpapillary image reconstructed from 3D OCT. INF = inferior; NAS = nasal; SUP = superior; TEMP = temporal; UHR = ultrahigh resolution.

The StratusOCT measures the NFL by acquiring a circumpapillary OCT image that is segmented to measure NFL thickness, with quantitative results displayed by quadrant, by clock hour, or as a graph. In the standard imaging protocol, 3 repeated circumpapillary scans of 3.4-mm diameter are acquired and statistics calculated from these 3 measurements.[33] Three repeated circumpapillary OCT images of 256 axial scans (transverse pixels) each can be acquired in 2 seconds, or 3 repeated higher pixel density images of 512 transverse pixels each can be acquired in 4 seconds. The 3.4-mm scan diameter was chosen to optimize measurement reproducibility and avoid overlap with the optic nerve head in the majority of eyes, while measuring an area where the NFL is relatively thick. Because the scanning speed of conventional OCT instruments is limited, only single-diameter circumpapillary scans are acquired, and NFL thickness data are available only along this scan.

Figure 6 shows a comparison between RNFL measurements performed using the GDx with variable corneal compensation, StratusOCT, and 3D OCT. The 3D OCT data enable the generation of an NFL thickness map (Fig 6g) similar to that obtained by the GDx, except that OCT measures the NFL thickness using cross-sectional image information, whereas the GDx measures the NFL thickness using birefringence. This map can provide information on radial and circumpapillary variations in the NFL thickness. Figure 6h shows a plot of the NFL thickness variation measured along a 3.4-mm circle centered about the optic disc. It is also possible to generate virtual OCT images that show a cross-sectional view of the retina along any line or contour. Circumpapillary OCT images of any diameter as well as radial OCT images can be generated. However, it is important to note that, because the raster scan protocol used in this example has an asymmetric axial scan spacing that is denser in the horizontal than the vertical direction, the circumpapillary OCT image has higher axial scan density in the segments along the horizontal direction than in those along the vertical direction. High-speed high-resolution OCT raster scanning was performed over a 6 × 6-mm area centered on the optic nerve head. Figure 6i shows an example of a 3.4-mm-diameter circumpapillary OCT image generated from the 3D OCT data. The virtual circumpapillary OCT image and the circumpapillary NFL thickness compare well with the circumpapillary OCT image and NFL thickness obtained using StratusOCT (Fig 6f, e).

Errors in circumpapillary NFL thickness measurement caused by blood vessels interfering with the segmentation algorithm can be identified and corrected using information from the OCT fundus image. Finally, OCT images and NFL maps can be precisely and repeatably registered to the fundus by using the OCT fundus image generated from the same 3D OCT data. This addresses a limitation in standard OCT in which variations in the scan position can produce variations in measured NFL thickness values. Therefore, we believe that the improved registration of OCT images and NFL maps with fundus features that is possible using 3D OCT should improve measurement reproducibility.

Characterization of the Optic Nerve Head

Characterization of optic nerve head topography and stereometric parameters such as the cup-to-disc (C/D) ratio is important for the diagnosis and monitoring of glaucoma. Clinical instruments for characterizing the optic nerve head include stereo fundus photography, the HRTII, RTA, and StratusOCT.

The HRTII functions similar to a scanning laser ophthalmoscope and acquires topographic information by performing a series of raster-scanned en face images at varying depths.[42] The HRTII can generate a series of 64 images consisting of 384 × 384 pixels in an acquisition time of 1.5 seconds. The HRTII enables comprehensive mapping of the contour of the optic nerve head as well as quantitative measurement of disc parameters (Fig 7a, b). Because the HRTII acquires fundus images in the measurement process, topographic information is precisely registered to fundus features.

The StratusOCT performs characterization of the optic nerve head using 6 intersecting 4-mm-long OCT images oriented in a radial pattern centered on the optic disc. Six images of 128 axial scans (transverse pixels) each can be acquired in ~2 seconds, or 6 images of 512 axial scans each can be acquired in ~10 seconds. The optic disc parameters are measured by software using an algorithm. The termination of the RPE and choriocapillaris near the lamina cribrosa is visible in the OCT images and is used as a landmark, and a line is constructed between the 2 termination points to define the disc diameter and a reference baseline for the orientation of the disc (Fig 7d). A line is then constructed parallel to this baseline and offset anteriorly by a given distance. The points at which this line intersects the vitreal retinal interface are then used to measure the cup diameter. These values are measured

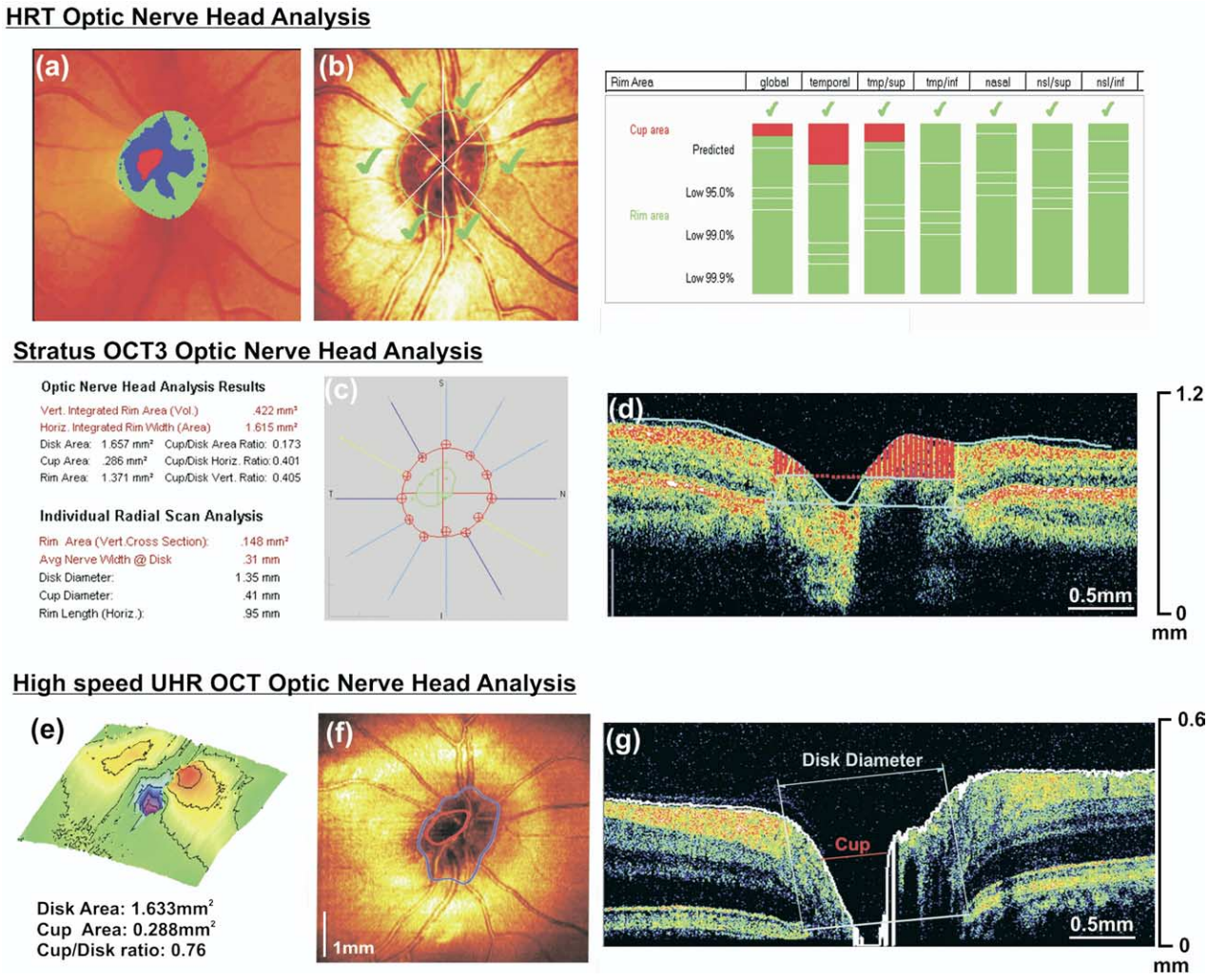

Figure 7. Comparison of optic nerve head analysis obtained by HRT, StratusOCT, and 3-dimensional optical coherence tomography (3D OCT) using high-speed ultrahigh-resolution (UHR) OCT imaging: **(a, e)** topographic maps of the optic nerve head from HRT and 3D OCT; **(b, c, f)** disc and cup contours from HRT, StratusOCT, and 3D OCT; **(d, g)** individual cross-sectional OCT images from StratusOCT and high-speed UHR OCT. inf = inferior; sup = superior.

on the 6 OCT images and used to calculate parameters such as vertical integrated rim area, horizontal integrated rim width, disc area, cup area, rim area, C/D area ratio, C/D horizontal ratio, and C/D vertical ratio.

The HRT and RTA require the operator to identify a contour line defining the optic disc around the nerve head rim. In StratusOCT, the termination of the RPE near the optic disc is used to determine the edge of the disc. However, the presence of shadowing caused by blood vessels can prevent fully automated analysis of OCT data, and operator assistance can be required. In addition, because only 6 OCT images are used, comprehensive mapping of disc topography is not obtained.

Quantitative topographic information on the optic nerve head can be obtained from 3D OCT data using high-speed UHR OCT. Figure 7 shows a comparison between optic nerve head analysis performed using the HRT, the StratusOCT, and 3D OCT. As shown in Figure 7a, c, HRT generates a topographic map of the optic nerve head and an image of the optic disc and performs quantitative measurements of disc parameters. StratusOCT (Fig 7c, d) generates a series of OCT images (1 of the 6 images is shown) and a 12-point map of the disc and cup and performs quantitative measurements of disc parameters. Three-dimensional OCT imaging was performed over a 6 × 6-mm area centered on the optic nerve head. Using 3D OCT data, it is possible to obtain comprehensive topographic and cross-sectional image information about the optic nerve head. Because full 3D data are available at a large number of transverse points in the optic nerve head region, much more information is available than with standard OCT, and image processing algorithm performance can be improved. Using 3D OCT, it is possible to identify and segment the RPE layer as well as the termination of the RPE in the central part of the optic disc region. Our algorithm automatically accounts for shadowing artifacts produced in the presence of retinal vessels and identifies the disc margins without the need for operator intervention. The disc margin is determined by averaging across an arc of the circular border to reduce perturbations from blood vessels. A topographic map of the retinal surface is generated using the RPE–choriocapillaris layer as a reference. This topographic surface information is used for automatic delineation of the cup contour. The edge of the cup is determined by the intersection of the retinal surface with a plane parallel to the RPE and offset by a given distance. The contours defining the cup and disc are then computed and displayed as an en-face map. The disc margin measured by StratusOCT appears smoother than that measured from 3D OCT data. However, it is important to note that the StratusOCT uses 6 radial OCT scans and, therefore, measures only 12 points on the disc margin. This results in a smoother but less accurate measurement.

Discussion

High-speed UHR OCT achieves axial image resolutions as fine as ~2 μm, a factor 5 times finer than standard OCT. Imaging speeds are up to 100 times faster than previous UHR OCT research systems and 40 times faster than the standard-resolution commercial StratusOCT. The high imaging speeds available with spectral/Fourier domain detection allow the acquisition of 3D OCT data. The number and density of axial scans on the retina are dramatically increased compared with standard OCT. This reduces sampling errors and reduces the possibility of missing focal pathologies. Three-dimensional OCT enables the generation of an OCT fundus image that precisely registers OCT images with fundus features. Optical coherence tomography fundus images of specific intraretinal layers or features can also be generated. Because 3D OCT data contain volumetric structural information on the retina, OCT images with arbitrary scan patterns, orientations, and positions can be generated, enabling comprehensive visualization and coverage of the retina. In addition, rendering and visualization techniques similar to those used in magnetic resonance imaging can also be applied.

Ultrahigh-resolution imaging enables improved visualization and segmentation of individual intraretinal layers relative to standard-resolution OCT. Ultrahigh-resolution 3D OCT enables quantitative mapping of the thickness of the retina, RNFLs, and photoreceptor layers. False-color thickness maps can be overlaid on the OCT fundus image. Furthermore, because morphometric data are registered precisely and reproducibly to features on the fundus, measurement variations arising from variations in OCT scan position should be significantly reduced, thereby improving the measurement reproducibility. Coupled with the improved axial resolution, this should provide more sensitive morphometric measurement that promises to enable earlier disease diagnosis and more sensitive characterization of disease progression.

Three-dimensional OCT can yield information similar to that from other commonly used imaging modalities. Using 3D OCT data, it is possible to obtain cross-sectional images as in StratusOCT, to map macular thickness as in the RTA, to measure NFL thickness as in the GDx, and to map optic nerve head topography as in the HRT. Further clinical studies are required to compare the performance of 3D OCT with these other imaging modalities.

The 3D OCT data used here were obtained with a raster scan pattern of 170 images, each consisting of 512 axial scans (transverse pixels), thus corresponding to a total of 87 000 axial scans. Each axial scan had 1024 axial pixels (in depth), so that the total 3D OCT data set was 170 × 512 × 1024. An asymmetric raster imaging protocol was chosen so that a series of high–transverse pixel–density images in the direction of the raster scan were obtained. However, many other scan protocols are possible. For example, a symmetric raster imaging protocol with 300 × 300 axial scans can be obtained in an acquisition time comparable to that of the protocol described here.

The acquisition time for the 3D OCT data shown in this article was 6 seconds, too long to avoid eye motion artifacts in many subjects. However, these results are preliminary, and further improvements in imaging speed are possible. We have rebuilt our research prototype recently and achieved data acquisition rates of 26 000 axial scans per second. This enables a reduction in the acquisition time of the 3D OCT data (87 000 axial scans) from 6 seconds to ~4 seconds. Faster acquisition times should be possible using higher-speed linescan camera technology. It is also important to mention that acquisition times can be reduced using current technology simply by acquiring fewer numbers of axial scans in the 3D data and trading off transverse pixel densities with image acquisition times. The 3D OCT described here was obtained over a 6 × 6-mm retinal area, but if a 3 × 3-mm area is measured, the acquisition time is 4

times faster. Furthermore, if ultrahigh axial resolution is not required, a linescan camera with 1024 pixels rather than 2048 can be used. This would reduce acquisition times by another 2 times, but would yield images with 512 axial pixels (2 camera pixels are required to generate 1 axial pixel) rather than 1024.

Although the 3D data sets are large, data compression algorithms, similar to those used for photography and video, can be applied to reduce the size of the data dramatically with virtually no loss in resolution, making efficient data storage and transmission possible.

A femtosecond laser light source was used in these studies to achieve ultrahigh axial image resolutions. Femtosecond laser sources have outstanding performance, but are expensive. They are useful for state-of-the-art research studies, in which achieving the highest possible image resolutions is important for understanding subtle changes of retinal morphology. However, superluminescent diode technology has improved dramatically recently, and axial image resolutions of 3.2 μm have been demonstrated.[43] These new superluminescent diode light sources are compact, robust, and less expensive than lasers, and promise to enable more widespread availability of UHR OCT imaging.

In this context, it is helpful to discuss briefly the relationship of technology research to future commercial availability. Commercial instrument manufacturers must make tradeoffs in performance versus cost, because the purpose of a commercial instrument is to enable access by the largest possible community. Furthermore, there are many other issues that must be addressed before a company can design and build an instrument. Thus, although next-generation commercial instruments will offer improvements in image resolution and speed, they will not provide the same levels of resolution and speed that are possible in a research prototype instrument.

The purpose of a research prototype is to perform studies at the very leading edge of the technology. This state-of-the-art technology can provide insight into fundamental research problems such as the structure and pathogenesis of retinal disease. These results can also help to define the specifications and protocols for the next generation of commercial technology. However, the performance of a research prototype does not reflect the next generation of commercial technology; rather, it reflects what can be ultimately achieved in the generation after the next generation.

In conclusion, 3D OCT imaging using high-speed UHR OCT promises to enable new retinal imaging and diagnostic protocols. The ability to obtain 3D volumetric OCT data will enable new methods of visualizing, mapping, and quantitatively measuring retinal structure and pathology. Improved image resolution, higher transverse pixel densities, and the ability to register precisely image information with fundus features should improve reproducibility of morphometric measurements. These advances in visualization and morphometry promise to yield not only a better understanding of disease pathogenesis, but also more sensitive diagnostic indicators of early disease and methods to assess disease progression and response to treatment.

Acknowledgment. The authors gratefully acknowledge the scientific contributions of M. Carvalho, who assisted in the development of the prototype research instrument used in this study; A. Kowalevicz and F. Kaertner, who developed the femtosecond lasers used in this study; and W. Drexler, for his early work on the development of UHR OCT. They also gratefully acknowledge collaboration with V. Shidlovski and S. Yakubovich of Superlum Diodes, Ltd.

References

1. Huang D, Swanson EA, Lin CP, et al. Optical coherence tomography. Science 1991;254:1178–81.
2. Hee MR, Izatt JA, Swanson EA, et al. Optical coherence tomography of the human retina. Arch Ophthalmol 1995;113:325–32.
3. Puliafito CA, Hee MR, Lin CP, et al. Imaging of macular diseases with optical coherence tomography. Ophthalmology 1995;102:217–29.
4. Hee MR, Fujimoto JG, Ko TH, et al. Interpretation of the optical coherence tomography image. In: Schuman JS, Puliafito CA, Fujimoto JG, eds. Optical Coherence Tomography of Ocular Diseases. 2nd ed. Thorofare, NJ: SLACK Inc.; 2004:21–53.
5. Podoleanu AG, Jackson DA. Combined optical coherence tomograph and scanning laser ophthalmoscope. Electron Lett 1998;34:1088–90.
6. Podoleanu AG, Seeger M, Dobre GM, et al. Transversal and longitudinal images from the retina of the living eye using low coherence reflectometry. J Biomed Opt 1998;3:12–20.
7. Yannuzzi LA, Ober MD, Slakter JS, et al. Ophthalmic fundus imaging: today and beyond. Am J Ophthalmol 2004;137:511–24.
8. Hitzenberger CK, Trost P, Lo PW, Zhou Q. Three-dimensional imaging of the human retina by high-speed optical coherence tomography. Opt Express [serial online] 2003;11:2753-61. Available at: http://www.opticsexpress.org/abstract.cfm?URI=OPEX-11-21-2753. Accessed October 20, 2003.
9. Drexler W, Morgner U, Krtner FX, et al. Invivo ultrahigh-resolution optical coherence tomography. Opt Lett 1999;24:1221–3.
10. Drexler W, Morgner U, Ghanta RK, et al. Ultrahigh-resolution ophthalmic optical coherence tomography. Nat Med 2001;7:502–7.
11. Drexler W, Sattmann H, Hermann B, et al. Enhanced visualization of macular pathology with the use of ultrahigh-resolution optical coherence tomography. Arch Ophthalmol 2003;121:695–706.
12. Ko TH, Fujimoto JG, Duker JS, et al. Comparison of ultrahigh- and standard-resolution optical coherence tomography for imaging macular hole pathology and repair. Ophthalmology 2004;111:2033–43.
13. Wollstein G, Paunescu LA, Ko TH, et al. Ultrahigh resolution optical coherence tomography in glaucoma. Ophthalmology 2005;112:229–37.
14. Schuman JS, Hee MR, Puliafito CA, et al. Quantification of nerve fiber layer thickness in normal and glaucomatous eyes using optical coherence tomography. Arch Ophthalmol 1995;113:586–96.
15. Hee MR, Puliafito CA, Duker JS, et al. Topography of diabetic macular edema with optical coherence tomography. Ophthalmology 1998;105:360–70.
16. Nassif NA, Cense B, Park BH, et al. In vivo high-resolution video-rate spectral-domain optical coherence tomography of the human retina and optic nerve. Opt Express [serial online] 2004;12:367-76. Available at: http://www.opticsexpress.org/

abstract.cfm?URI=OPEX-12-3-367. Accessed February 9, 2004.
17. Leitgeb RA, Drexler W, Unterhuber A, et al. Ultrahigh resolution Fourier domain optical coherence tomography. Opt Express [serial online] 2004;12:2156-65. Available at: http://www.opticsexpress.org/abstract.cfm?URI=OPEX-12-10-2156. Accessed May 17, 2004.
18. Wojtkowski M, Srinivasan VJ, Ko TH, et al. Ultrahigh-resolution, high-speed, Fourier domain optical coherence tomography and methods for dispersion compensation. Opt Express [serial online] 2004;12:2404-22. Available at: http://www.opticsexpress.org/abstract.cfm?URI=OPEX-12-11-2404. Accessed May 30, 2004.
19. Wojtkowski M, Bajraszewski T, Gorczynska I, et al. Ophthalmic imaging by spectral optical coherence tomography. Am J Ophthalmol 2004;138:412–9.
20. Ergun E, Hermann B, Wirtitsch M, et al. Assessment of central visual function in Stargardt's disease/fundus flavimaculatus with ultrahigh-resolution optical coherence tomography. Invest Ophthalmol Vis Sci 2005;46:310–6.
21. Fercher AF, Hitzenberger CK, Kamp G, Elzaiat SY. Measurement of intraocular distances by backscattering spectral interferometry. Opt Commun 1995;117:43–8.
22. Hausler G, Lindner MW. Coherence radar and spectral radar-new tools for dermatological diagnosis. J Biomed Opt 1998; 3:21–31.
23. Wojtkowski M, Leitgeb R, Kowalczyk A, et al. In vivo human retinal imaging by Fourier domain optical coherence tomography. J Biomed Opt 2002;7:457–63.
24. Wojtkowski M, Bajraszewski T, Targowski P, Kowalczyk A. Real-time in vivo imaging by high-speed spectral optical coherence tomography. Opt Lett 2003;28:1745–7.
25. Nassif N, Cense B, Park BH, et al. In vivo human retinal imaging by ultrahigh-speed spectral domain optical coherence tomography. Opt Lett 2004;29:480–2.
26. Swanson EA, Izatt JA, Hee MR, et al. In vivo retinal imaging by optical coherence tomography. Opt Lett 1993;18:1864–9.
27. Tearney GJ, Bouma BE, Boppart SA, et al. Rapid acquisition of in vivo biological images by use of optical coherence tomography. Opt Lett 1996;21:1408–10.
28. Tearney GJ, Brezinski ME, Bouma BE, et al. In vivo endoscopic optical biopsy with optical coherence tomography. Science 1997;276:2037–9.
29. Swanson EA, Huang D, Hee MR, et al. High-speed optical coherence domain reflectometry. Opt Lett 1992;17:151–3.
30. Leitgeb RA, Hitzenberger CK, Fercher AF. Performance of Fourier domain vs. time domain optical coherence tomography. Opt Express [serial online] 2003;11:889-94. Available at: http://www.opticsexpress.org/abstract.cfm?URI=OPEX-11-8-889. Accessed April 21, 2003.
31. de Boer JF, Cense B, Park BH, et al. Improved signal-to-noise ratio in spectral-domain compared with time-domain optical coherence tomography. Opt Lett 2003;28:2067–9.
32. Choma MA, Sarunic MV, Yang C, Izatt JA. Sensitivity advantage of swept source and Fourier domain optical coherence tomography. Opt Express [serial online] 2003;11:2183-9. Available at: http://www.opticsexpress.org/abstract.cfm?URI=OPEX-11-18-2183. Accessed September 8, 2003.
33. Schuman JS, Pedut-Kloizman T, Hertzmark E, et al. Reproducibility of nerve fiber layer thickness measurements using optical coherence tomography. Ophthalmology 1996;103: 1889–98.
34. Podoleanu AG, Rogers JA, Jackson DA, Dunne S. Three dimensional OCT images from retina and skin. Opt Express [serial online] 2000;7:292-8. Available at: http://www.opticsexpress.org/abstract.cfm?URI=OPEX-7-9-292. Accessed October 23, 2000.
35. Podoleanu AG, Dobre GM, Cucu RG, et al. Combined multiplanar optical coherence tomography and confocal scanning ophthalmoscopy. J Biomed Opt 2004;9:86–93.
36. Zeimer R, Asrani S, Zou S, et al. Quantitative detection of glaucomatous damage at the posterior pole by retinal thickness mapping. A pilot study. Ophthalmology 1998;105:224–31.
37. Zeimer RC, Mori MT, Khoobehi B. Feasibility test of a new method to measure retinal thickness noninvasively. Invest Ophthalmol Vis Sci 1989;30:2099–105.
38. Zeimer R, Shahidi M, Mori M, et al. A new method for rapid mapping of the retinal thickness at the posterior pole. Invest Ophthalmol Vis Sci 1996;37:1994–2001.
39. Polito A, Shah SM, Haller JA, et al. Comparison between retinal thickness analyzer and optical coherence tomography for assessment of foveal thickness in eyes with macular disease. Am J Ophthalmol 2002;134:240–51.
40. Medeiros FA, Zangwill LM, Bowd C, Weinreb RN. Comparison of the GDx VCC scanning laser polarimeter, HRT II confocal scanning laser ophthalmoscope, and Stratus OCT optical coherence tomograph for the detection of glaucoma. Arch Ophthalmol 2004;122:827–37.
41. Dreher AW, Reiter K, Weinreb RN. Spatially resolved birefringence of the retinal nerve fiber layer assessed with a retinal laser ellipsometer. Appl Opt 1992;31:3730–5.
42. Weinreb RN, Dreher AW, Bille JF. Quantitative assessment of the optic nerve head with the laser tomographic scanner. Int Ophthalmol 1989;13:25–9.
43. Ko TH, Adler DC, Fujimoto JG, et al. Ultrahigh resolution optical coherence tomography imaging with a broadband superluminescent diode light source. Opt Express [serial online] 2004;12:2112–9. Available at: http://www.opticsexpress.org/abstract.cfm?URI=OPEX-12-10-2112. Accessed May 17, 2004.